KAPL-P-000124
(K98168)

FABRICATION AND ELECTRICAL CHARACTERIZATION OF 0.55 eV N-on-P InGaAs THERMOPHOTOVOLTAIC DEVICES

CONF-981055--

W. Nishikawa, G. Charache

October 1998

DISTRIBUTION OF THIS DOCUMENT IS UNLIMITED

MASTER

NOTICE

KAPL ATOMIC POWER LABORATORY SCHENECTADY, NEW YORK 12401

Operated for the U. S. Department of Energy
by KAPL, Inc. a Lockheed Martin company

FABRICATION AND ELECTRICAL CHARACTERIZATION OF 0.55eV N-ON-P InGaAs TPV DEVICES

W.Nishikawa, D. Joslin, D.Krut, J. Eldredge, A. Narayanan*, M. Takahashi, M.Haddad, M. M. Al-Jassim **and N.H. Karam

Spectrolab Inc., Sylmar, CA
*HRL Laboratories L.L.C., Malibu, CA
** National Renewable Energy Laboratory, Golden, CO

Abstract:

Results are presented on the characterization and testing of lattice mismatched 0.55 eV InGaAs/InP thermophotovoltaic (TPV) cells. A robust cell fabrication technique amenable to high throughput production is presented. A versatile light and dark I-V set up capable of fast screening of the TPV cells and an innovative approach for screening high performance cells are presented. We also report on the effect of lattice matched InAsP and InAlAs back surface field on the performance of the TPV cells.

Introduction:

Thermophotovoltaic (TPV) energy generation involves direct conversion of infra-red, thermal radiation into electrical energy via photovoltaic (PV) response in semiconductors. Proposed in 1961 [1], strong resurgence in TPV systems has recently arisen based on the demand for self-contained power sources and on technological developments in InGaAs and GaSb tandem solar cells. Current TPV systems have focused on low-temperature blackbody emitters between 1000°C - 1500°C where direct low-bandgap PV cells and system hardware can operate practically. Ternary InGaAs and quarternary InGaAsSb material systems have been engineered to match emitter peak wavelengths between 1.9-2.6 μm.

Our TPV research has focused on n-on-p 0.55eV InGaAs-based devices with a targeted emitter peak at $\lambda_g = 2.25\mu m$. Material research has studied controlling defects in InGaAs step-graded structures and at back surface interfaces. For high throughput production, a device structure is grown with an optically transparent cap layer benefitting from reduced processing steps. For 1cm^2 cells, we report external quantum efficiency (EQE) performance above 55% at $\lambda = 2.0\mu m$, open-circuit voltage (V_{oc}) between 290mV-300mV, and short-circuit (I_{sc}) values of ~3.0A/cm^2. Correlations between V_{oc}, EQE, and dark currents have been established for charting device improvement.

Material Growth and Characterization:

The lattice mismatched InGaAs/InP TPV device structures were grown using a vertical, rotating-disk low-pressure Metal Organic Vapor Phase Epitaxy (MOVPE) reactor. Films were grown on p-type (3-5 x10^{18} cm^{-3}) InP substrates with direct (100) and 2° off (100) → [110] orientations. A schematic of the TPV device structure is shown in Figure 1.

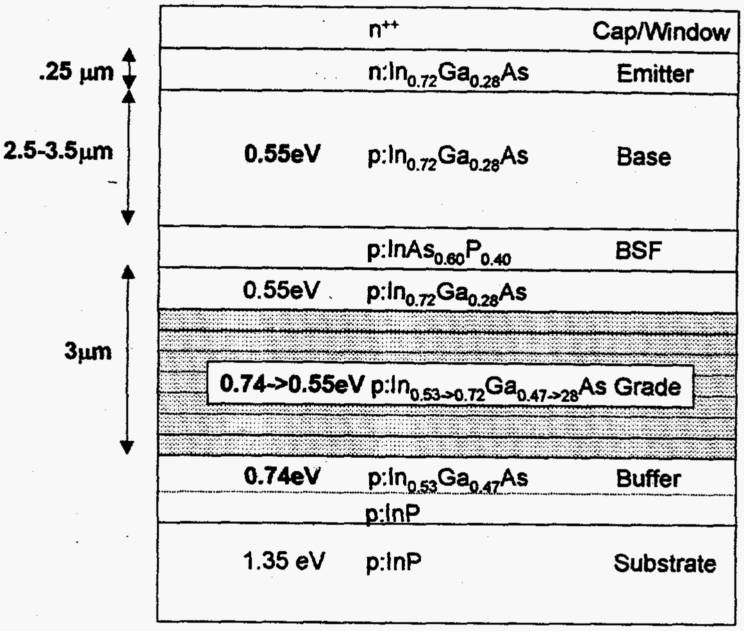

Figure 1. Schematic of optimized TPV structure

A step-graded buffer was used to accommodate the lattice-mismatch between the 0.74 eV $In_{0.53}Ga_{0.47}As$ on InP and the 0.55 eV $In_{0.72}Ga_{0.28}As$. The step-graded structure is designed to introduce uniform misfit dislocations at each step and prevent them from threading to the active device region. Figure 2 shows a cross-sectional transmission electron microscopy (XTEM) image of the full device structure, where the dislocations are deflected parallel to the step-graded layers and away from the active region of the device. The surface morphology of good devices had a fine, cross-hatched appearance, as expected from relaxed layers.

The n-on-p device structures had a base layer thickness in the range of 2.5 -3.5µm and n-emitter thickness ~.25µm. A heavily-doped cap was grown as the last step to form an ohmic contact. The Moss-Burstein shift caused by heavy Sn doping ($>3.0\times10^{19}$ cm^{-3}) provided an optical transparency, in wavelength range below the InGaAs bandgap, which simplifies cell processing and improves emitter surface recombination [2].

It is critical to lattice-match the back surface field (BSF) to the 0.55eV InGaAs base layer. Although it is easier to grow $In_{0.72}Al_{0.28}As$ lattice matched to 0.55 eV InGaAs than $InAs_{0.4}P_{0.6}$, the latter is the preferred BSF choice. Oxygen incorporation in Al containing layers is problematic as it increases interfacial defects and back surface recombination. Figure 2b shows a XTEM of a lattice matched $InAs_{0.4}P_{0.6}$ BSF to 0.55 eV InGaAs base.

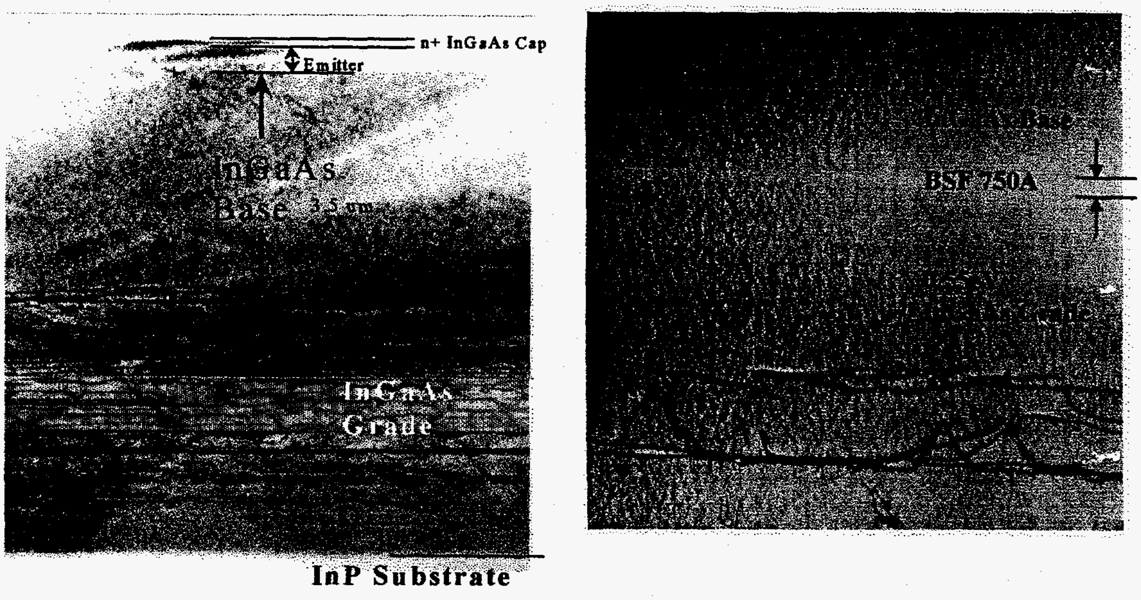

(a)

(b)

Figure 2: XTEM image of a full TPV device structure without a BSF (a), and a higher magnification XTEM illustrating $In_{0.72}Ga_{0.28}As$ Base/$In_{0.40}As_{0.60}P$ BSF interface (b).

TPV Device Fabrication Process:

The conventional device fabrication process for TPV and most other photovoltaic devices involves formation of front and back contacts, deposition of anti-reflection coating (if required), and cell isolation. Typically, front-side grid deposition necessitates a two-step photolithographic process of: 1) masking and etching the optically-absorbing cap layer outside of the grid lines, and 2) depositing front metal and forming the grid lines via a lift-off process. On the backside, a low-resistance substrate contact must be formed to mitigate the I^2R power losses, which become more severe at high current densities. Forming reliable ohmic contacts to p-type InP is difficult since Zn-doped InP substrates doped greater than $3x10^{18}$ cm^{-3} are not readily available.

We have developed a manufacturable process for TPV cells streamlining both front and back contact steps. From 2-inch InP wafers, twelve 1cm x 1cm cells were fabricated. Following MOVPE growth, back contacts to the InP substrates (Zn-doped ~$3x10^{18}$) were sequentially sputtered Au/Zn/Au, where the composition was determined by respective layer thickness. The initial Au nucleation layer enhanced the Zn doping at the surface [3]. Contact sintering catalyzed Au_2P_3 formation at the semiconductor/metal interface. Specific contact resistances in the range of $1x10^{-4}$ Ohms-cm^2 were achieved for two temperature conditions at 410°C and 430°C, as shown in Figure 3. Visually, the back contact appeared matte with a pink color, indicative of the Au_3In phase at the metal surface.

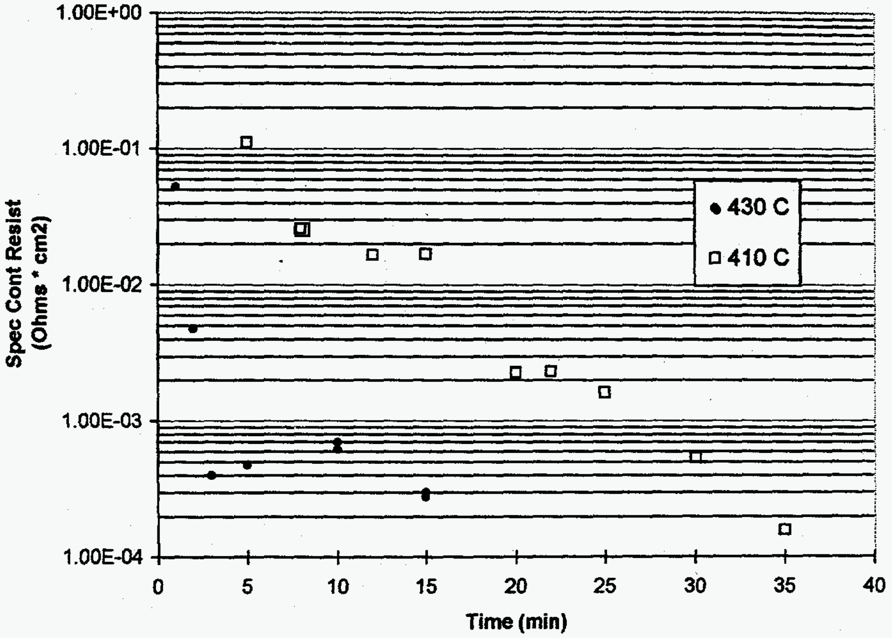

Figure 3: Au/Zn/Au Back Contact Optimization to P-Type InP Substrates

Benefiting from the optical properties of the n^{++} cap layer, the front-side processing required only one photomask to define front-metal grids. Narrowly-spaced 10µm grid lines were defined using a two-layer resist process to increase resist to metal aspect ratio and improve lift-off profiles.

A non-alloyed Cr/Au/Ag contact is easily achieved for the front contact. Metal adhesion to InGaAs can be improved by short sintering. The majority of the metal thickness was contained in the Ag layer (>5 µm). To complete the TPV fabrication sequence, individual cells were saw-diced rather than mesa isolation. This eliminated another photolithography step and etch process.

Cell processing of full devices is routinely accomplished in a single day using this process, compared to the two-day conventional process.

Electrical Testing

Full electrical characterization of devices included in-house measurements of light I-V, dark I-V, and cell spectral response (SR) or EQE. Spectral reflectance measurements were also taken on selected samples to convert EQE to internal quantum efficiency (IQE).

An innovative pulsed-light I-V system was developed for fast and easy characterization of the TPV cells. Figure 4 is a schematic of the test station designed to produce the necessary current generation in the test TPV device to simulate real system performance. The light generation was provided by a tungsten-halogen light source with a gold-coated, non-image forming reflector. A long-pass filter with a cutoff at 1µm was implemented to remove the visible and some near-IR light that is not found in the1000°C blackbody spectrum.

The custom fixture was designed for a "true" 4-point probe measurement to prevent back contact problems and non-destructive testing of TPV cells. Spectrolab designed an automated cell evaluation (ACE) data acquisition system capable of measuring high current levels up to 5 amps with sweep rates in the 100ms range which was used for rapid collection of light and dark IV curves.

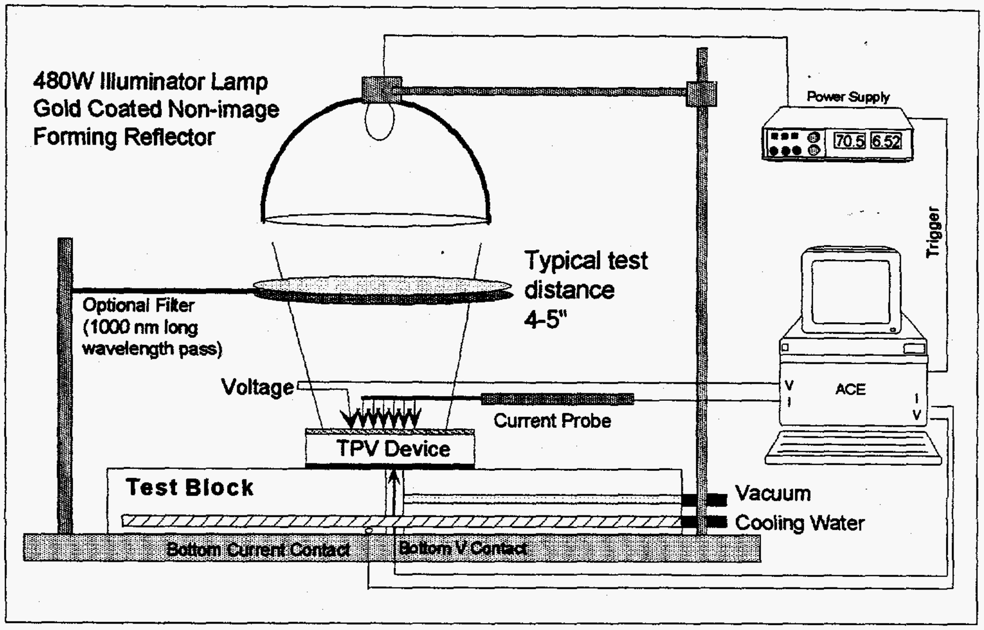

Figure 4: TPV Light-IV Test Station with Test Fixture

To avoid thermal heating problems, the device-under-test (DUT) is exposed to a short (~1sec) illumination and the IV response is swept over 100ms. The light source intensity is allowed to reach its maximum and no significant heating of the cell is observed.

Cells are first tested using an in-house SR/EQE system in the range between 900nm and 2300nm at 25nm intervals. EQE measurements are not only valuable tools in measuring and isolating problematic areas in the cell structure, but also provide the integrated Jsc value for devices tested under high concentration conditions. Standard test procedures set light intensity to generate between 3- 3.3A (3.15 nominally) for cells exhibiting near "respectable" QE performance. For cells with below-normal QE, light intensity for the light IV test is adjusted to generate somewhat lower current in the device.

Device Performance Results:

High performance TPV devices are easily achievable in the lattice mismatched 0.55 eV InGaAs/InP TPV cells by optimizing the diffusion length in the base and carefully passivating the front and back side of the cell. The BSF/base interface is critical to efficient carrier collection and high EQE. Figure 5 shows a comparison of the EQE for cells grown with lattice matched InAsP, InAlAs and without a BSF. The 1cm^2 cells of wafer SPL#1 with InAsP BSF produced the highest EQE values peaking at 56.7% at 2.0 µm. These measurements are comparable to the highest reported EQE values reported for 0.55eV InGaAs devices [4]. Base and BSF thickness optimizations were guided by the EQE response at 2.0µm. The motivation of a thinner base was the enhancement of the BSF effectiveness and reduction of dark current volumes. As described in the next section, strong correlation between lower dark current (I_{dark}) levels and increased V_{oc} performance has been established. To prevent generation of threading dislocation networks at the base interface, BSF thickness was varied to ensure that the InAsP layer was psuedomorphic. Thinning the BSF allowed greater tolerance for matching InAsP composition to the 0.55eV InGaAs lattice constant. Optimized devices were grown with InAsP BSF layers below 1000Å. For all devices, the lower EQE characteristic at short wavelength can be attributed to discrepancies in the reflection characteristics of the reference cell.

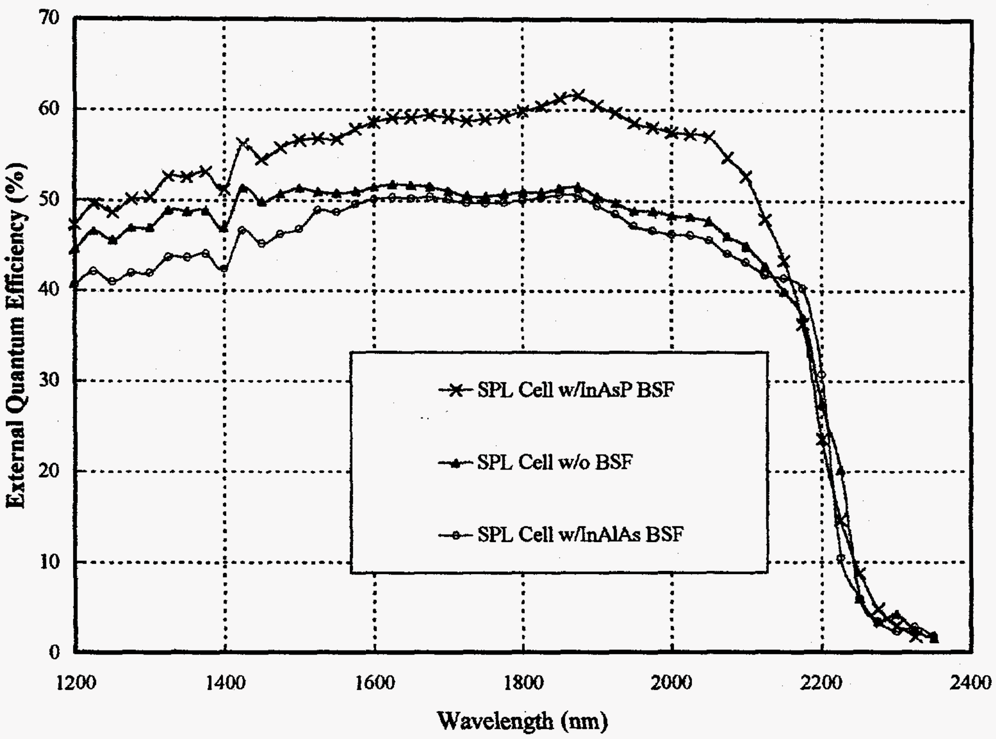

Figure 5. External QE Measurements of Spectrolab (SPL) 0.55eV InGaAs TPV cells.

Figure 6 displays light I-V curves for TPV devices with V_{oc} outputs up to 301mV at J_{sc} between 3.0-3.7 A/cm^2. Concentrated light testing was done under 1000nm filtered conditions. It has been verified that using the short wavelength filter improved open circuit voltages ~ 5mV due to the increased carrier injection deeper in the device near the BSF.

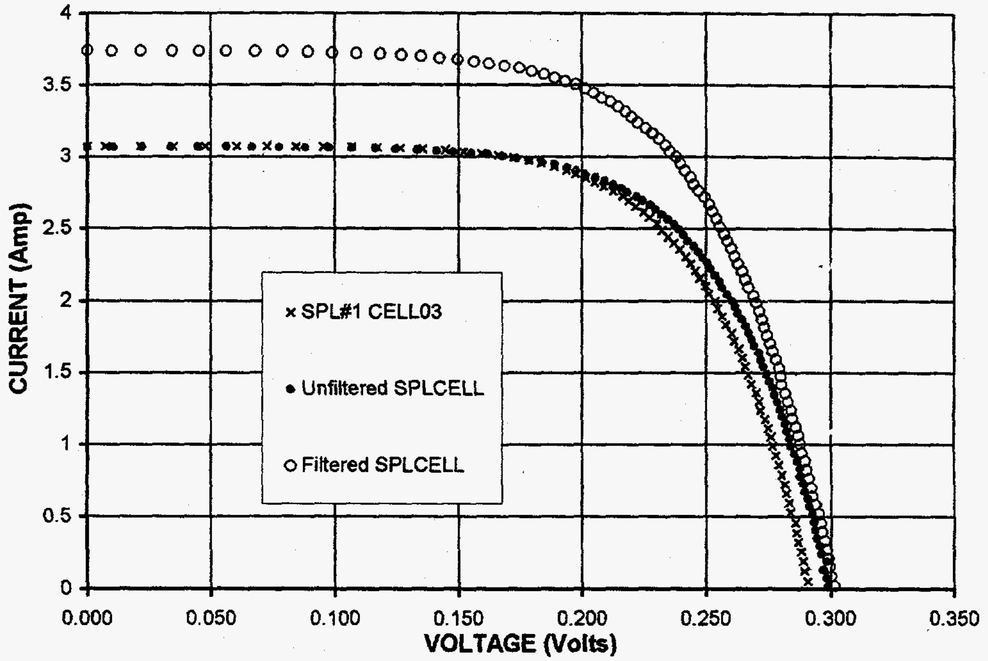

Figure 6. Light I-V Measurements of Spectrolab 0.55eV InGaAs TPV cells.

Empirical Device Analysis

The EQE, light I-V, and dark I-V results can be correlated to provide insight as to what portions of the device are most important to output. Data from the dark I-V characteristic, where the current is measured over several orders up to 3 A/cm^2, can be fit by the simple diode equation. By using a least squares technique to perform this fit, the ideality factor (*n*), the reverse saturation current (I_o), and the grouped series resistance (R_{series}) terms can be extracted. The simple form of the diode equation is given by

$$I = I_o \exp\frac{q(V + I \cdot R_{series})}{n \cdot k \cdot T} - 1 \qquad [1.1]$$

We have calculated the R_{series} to be approximately 3 milliohms (mΩ)-cm^2 for 1x1 cm fully processed cells with Au/Zn/Au back contacts. For purposes of comparison, it can be shown from numerical simulation of the light I-V characteristic that R_{series} value of 10 milliohm-cm^2 will reduce output of the device by 10.5% and must be kept below 5 mΩ-cm^2 to reduce power loss.

We have developed a method of data analysis correlating EQE at 2000 nm, V_{oc} from the light I-V curve, and I_{dark} at 0.2 volts from the dark I-V data to TPV cell performance. When the diode expression is evaluated under illumination at open circuit, it can be shown that

$$\ln(I_o) = \ln(I_{sc}) - \frac{q \cdot V_{oc}}{n \cdot k \cdot T} \qquad [1.2]$$

If I_{sc} is held constant in equation 1.2, the natural logarithm of the reverse saturation current I_o can be plotted versus the open circuit voltage. From dark I-V response, I_o is proportional to the device dark current at a given voltage (I_{dark} at 0.2 voltage near load), assuming that series and shunt components are negligible. When the ideality factor for various devices is similar, I_{dark} values may be compared and taken as a metric for I_o.

In Figure 7, I_{dark} at 0.2V is plotted against V_{oc} correlating high V_{oc} output to low I_{dark} currents in devices. For purposes of comparison, the data was fit for several Spectrolab devices and plotted over the voltage range that included the V_{oc} of benchmark devices. The best device SPL#1 Cell03, shown in Figure 6 with V_{oc} of 291 mV, had I_{dark} of 0.07A/cm^2 at 0.2V.

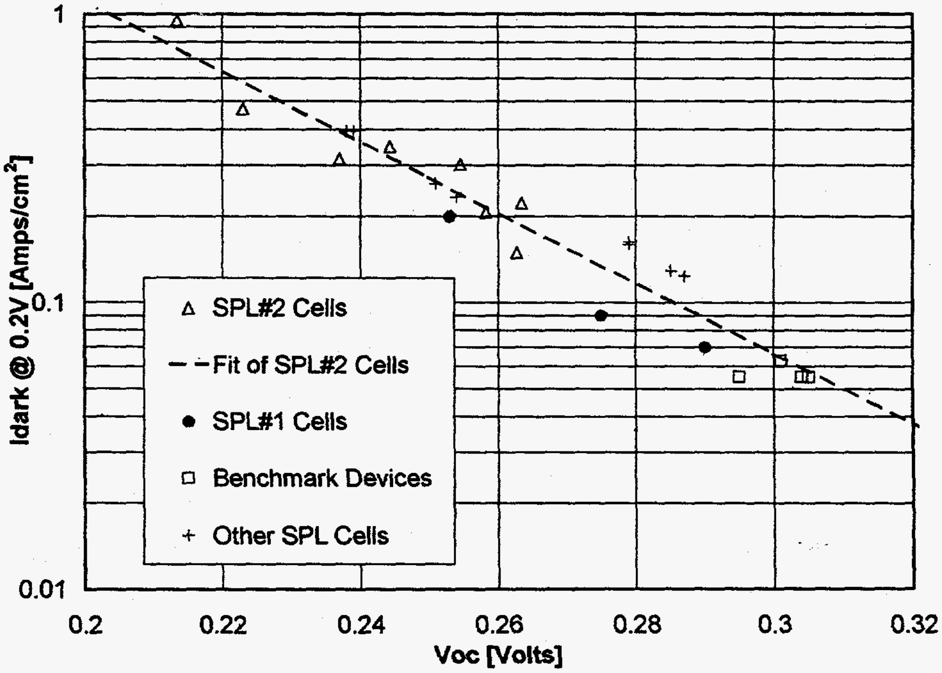

Figure 7. Semi-log Plot of Idark at 0.2V versus Voc

In a similar fashion, EQE data can be correlated to the I_o (or I_{dark}) parameters. From one-dimensional transport equations, QE or current generation can be derived as a function of diffusion length (L_n) assuming a semi-infinite absorber (base thickness) [5]. Since the saturation current I_o is inversely proportional to L_n, the QE function can be approximated as directly proportional to 1/(1+I dark). In Figure 8, the results are plotted for the same devices described in Figure 7. SPL#1 Cell03 yielded the highest EQE measured at 57.6% corresponding to the highest V_{oc} at 291 mV and lowest I_{dark} of that wafer. These diagnostic methods were valuable in predicting necessary EQE performance levels and I_{dark} values by linear-regression extrapolations.

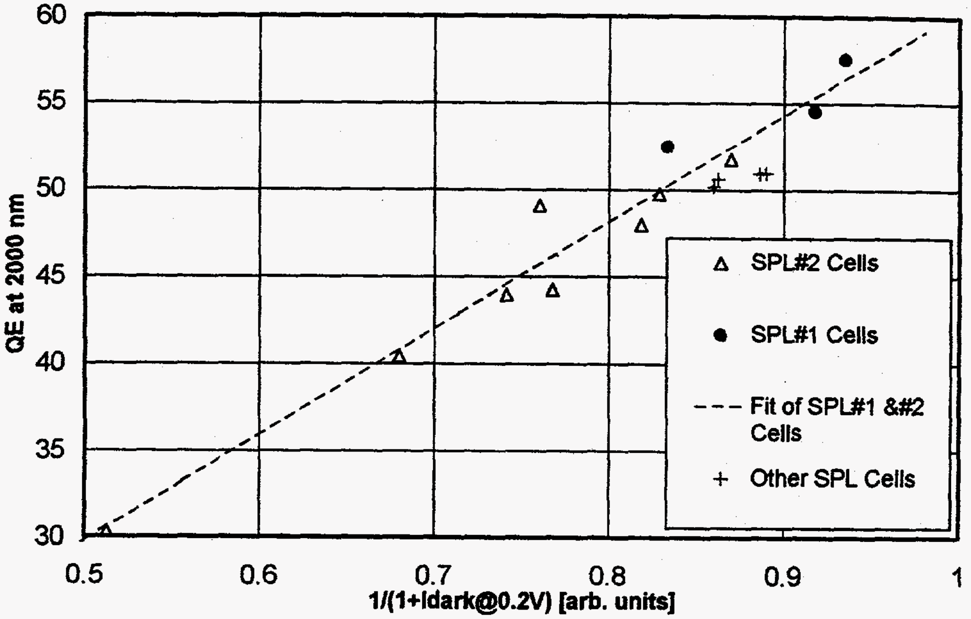

Figure 8. Plot of EQE at 2000nm versus 1/(1+Idark) for Spectrolab devices

The implication from these analysis methods is that current collection from deeply absorbed photons is improved with low I_o values. These low I_o values are shown to correlate strongly with high V_{oc} performance. When EQE at 2.0μm and V_{oc} is high, the corresponding device efficiency will also be high. This reduces sole dependence on light I-V measurement to assess whether a given device performs well. However, these plotted relationships cannot reveal certain material characteristics such as diffusion length or back surface recombination. Both EQE and V_{oc} losses are controlled by short diffusion lengths and high interface recombination generated from defected material and high I_o values. For this assessment XTEM and related material characterization techniques such as time-resolved photo-luminescence gather more direct information.

Summary:

Device processing and electrical characterization techniques for 0.55eV InGaAs TPV cells on InP were investigated. InAsP BSF layers have shown to obviate oxygen gettering and improve interface quality. The device structure, with the heavily-doped cap layer, offered the advantage of 1-mask processing and high throughput manufacturing. Full electrical testing (light I-V, dark I-V, EQE) was taken to understand how sections of the device operate. The link between reduced dark current levels and improved Voc and EQE was formulated. The optimization of base diffusion length and passivating the front and back of the device lead to EQE above 55% and V_{oc} of 301mV. Plotting dark current values against V_{oc} and EQE have been effectively used to gauge device performance gauge and to extrapolate targeted cell outputs.

References:

[1] P. Aigrain, The thermo-photovoltaic converter, Unpublished lectures given at the Dept. of Electrical Engineering, Massachusetts Institute of Technology, 1960-1961.

[2] G. Charache, D. Depoy, et. al.,"Electrical and optical properties of degenerately-doped n-type InxGa1-xAs," 3rd NREL TPV Conference Proceedings, CIP 401, p.215.

[3] V. Malina, V. Micheli, et. al.,"Effect of deposition parameters on the electrical metallurgical properties of Au-Zn contact to p-type InP," Semicond. Sci. Techno., 9, 1994,pp. 1523-1528.

[4] S. Wojtczuk, P. Colter, G. Charache, et. al. "Production data on 0.55eV InGaAs thermophotovoltaic cells,: Proc. 25th IEEE Photovoltaic Specialist Conference, 1996, pp. 77-80.

[5] A. Fahrenbrush and Richard Bube, *Fundamentals of Solar Cells*, New York: AP, 1983, p. 85.